Flux profile scanners for scattered high-energy electrons

R. S. Hicks[a,1], P. Decowski[b,*], M. Breuer[a,2], E. Chudakov[c], C. Arroyo[a], J. Celli[a,3], K. Pope[b,4], J. Ricci[a], J. Savage[a], M. Olson[d,5], K. Kumar[a], G.A. Peterson[a], and P. Souder[e]

[a] *University of Massachusetts Amherst, Amherst, MA 01003, USA*

[b] *Smith College, Northampton, MA 01063, USA*

[c] *Thomas Jefferson Laboratory, Newport News, VA 23606, USA*

[d] *Stanford Linear Accelerator Center, Menlo Park, CA 94025, USA*

[e] *University of Syracuse, Syracuse, NY 13244*

Received_____Accepted_____

Abstract

The paper presents a discussion of the design and performance of flux integrating Cerenkov scanners with air-core reflecting light guides used in a high energy, high flux electron scattering experiment at the Stanford Linear Accelerator Center. The scanners were highly radiation resistant and provided good signal to background ratios leading to very good spatial resolution of the scattered electron flux profile scans.

PACS: 29.40.Ka

Keywords: Electron flux profile scanner, Cerenkov detector, air-core reflecting light guide

[*] Corresponding author. Department of Physics, Smith College, Northampton, MA, 01063, USA, Tel: 413 585 3882, Fax: 413 585 3786

E-mail address: pdecowski@smith.edu

[1] Present address: 5037 Great Ocean Rd., Lavers Hill, Victoria, Australia 3238

[2] Present address: 97 Mt. Warner Rd., Hadley, MA 01035, USA.

[3] Present address: Physics Dept., 590 Commonwealth Ave., Boston University, Boston, MA 02215, USA.

[4] Deceased.

[5] Present address: St. Norbert College, De Pere, WI 54115, USA.

1. Introduction

Electron-electron (Møller) scattering at GeV beam energies gives rise to a far-forward angular distribution of scattered electrons. If hydrogen targets are used, small angle electron scattering from protons must be distinguished from the electron-electron

scattering. This report describes detectors built to measure the spatial distribution and relative integral flux of scattered electrons from intense incident beams of 48.3 and 45.0 GeV electrons incident upon a liquid hydrogen target in the E158 experiment at the Stanford Linear Accelerator Center [1].

The detector design confronted two main challenges. First, the intensity of the scattered electron flux of interest (4 GHz at a duty cycle of $5*10^{-5}$) created a very harsh radiation environment. This precluded the use of components that would be exposed for significant periods to the scattered beam, including photomultiplier tubes. Second, within the scattered beam the particle flux varied by more than an order-of-magnitude. The detector therefore needed to have fine granularity without being influenced by the magnitude of the flux nearby.

The active detector element was fused-silica that produced Cerenkov light and was preceded by a tungsten pre-radiator. Such detectors are not only radiation-hard, but they also have a directional response that can be exploited to suppress background. Cerenkov light from the fused silica was directed by means of a reflective air-core light-guide to a photomultiplier tube (pmt) safely located outside the scattered beam, 50 cm from the radiator. Conventional solid light-guide materials were unacceptable. Such light guides would produce abundant Cerenkov light and could scintillate. Furthermore, they would degrade or discolor because of the intense radiation background. The light produced inside such light guides could exceed the small signal produced when the detector's active element–but not the light guide–is located in a region of relatively low scattered-beam intensity. The air-core light guides we developed consisted of hollow-tubes lined with reflective Alzak sheet [2]. Alzak has an optical finish produced by electrochemically brightening and anodizing a high purity aluminum alloy. It also has high permanent reflectivity and good resistance to corrosion and abrasion.

These detectors were mounted on electromechanical movers that allowed the detector element to be moved remotely through the scattered beam. In one application this enabled us to determine the full spatial profile of the scattered beam intensity. Of course, the same result could also have been achieved by using an array of detectors and light-guides. However, this would have required periodic cross-calibrations of the responses of the various detectors. The use of a single, or, at most, a small number of scanning detectors not only avoided this chore, but also facilitated the removal of the detectors from the scattered beam profile during data acquisition with other detectors.

These detectors were developed for SLAC experiment E158 [1] whose objective was to determine the weak mixing angle by the measurement of parity-violation in the Møller scattering of polarized electrons from electrons in a liquid hydrogen target. This experiment employed a forward spectrometer, and the polarization asymmetry of the Møller cross section was determined by flux-integration of the forward-scattered electron beams of different helicities. Due to the design of the E158 spectrometer, scattered electrons were constrained to two forward-directed circular bands between 4.4 and 7.5 mr surrounding an intense background of forward photons generated by bremsstrahlung within the target. Near the main E158 calorimeter detector, the radial distribution of the scattered electron ranged from 18–35 cm, with Møller electrons confined to an inner band of radius 18–24 cm containing about 2×10^7 electrons per beam pulse. Outside the Møller band was a concentric band of electrons produced by the scattering of the incident

electrons off the protons in the hydrogen target. During data collection a collimator was positioned to intercept these electrons before they were absorbed in the calorimeter.

2. Small-probe Cerenkov detectors

2.1 General Discussion

The primary function of these detectors was to carefully map the relative spatial distribution of the scattered beam before it was absorbed in the Møller calorimeter. This mapping constituted the principal means of ensuring that the beam was centrally aligned at the detector, and that the inner ring of Møller electrons was clearly separated from the outer ring of Mott electrons. If the beam profile was found to be unsatisfactory, beam steering adjustments were made upstream of the target.

Figure 1 illustrates the essential features of these detectors. The active element was a 5 x 5 x 20 mm^3 piece of fused silica. This was oriented at an angle of 45° with respect to the incident beam in order to match the Cerenkov angle for relativisitic electrons in fused silica. In order to increase the sensitivity of the device, a rhombic 5 x 15 x 15 mm^3 tungsten pre-radiator was mounted on the upstream side of the radiator. Cerenkov photons emerging from the end of the radiator were reflected along a tube lined with a reflective Alzak [2] foil until they were detected by a photomultiplier tube (pmt).

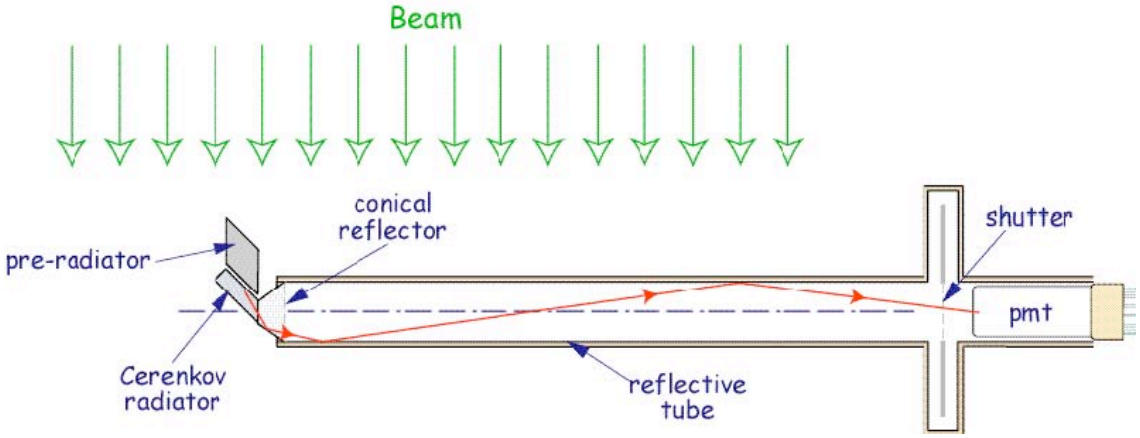

Fig. 1. Schematic layout for measuring the spatial distribution of a broadly distributed intense beam. Cerenkov photons produced in the radiator are reflected to a remotely located photomultiplier tube (pmt) by means of a air-core light guide. By closing the shutter, a measurement can made of the background produced by ionizing radiation striking the pmt.

2.1 Design Considerations

Extensive Monte-Carlo simulations were made to optimize the design of the detector. These revealed that even though the fused silica radiator was aligned to match the opening angle of the Cerenkov light cone, the overwhelming majority of detected Cerenkov photons were multiply reflected inside the radiator. Because not all of these reflections proceeded by total internal reflection, wrapping the radiator in reflective foil

increased the sensitivity of the device by about 10%.

Due to the multiple reflections inside the radiator, Cerenkov photons emerge from the end of the radiator with a large range of angles. Simulations showed that a reflector cone surrounding the end of the radiator would be effective in deflecting Cerenkov photons towards the pmt, thereby increasing the sensitivity of the device.

Two provisions were made to help identify and determine experimental backgrounds. First, as indicated in Fig. 1, an electromechanical shutter was installed immediately in front of the pmt. With the shutter open, reflected Cerenkov photons could enter the pmt and interact in its photocathode. When shut, however, the shutter intercepted those photons permitting a measurement of the background due to ionizing radiation hitting the pmt. The second provision, not indicated in Fig. 1, was the capability of being able to move the pre-radiator from the upstream to the downstream side of the radiator. This allowed us to ensure that the signal was due to the beam directly striking the pre-radiator, rather than from secondary interactions of the beam in other nearby components of our experimental setup.

The key variables affecting the sensitivity were the internal diameter and length of the reflector lined tube, and the properties of the radiator, pre-radiator, and reflecting surfaces. One concern was that rolling the Alzak sheet to form a small-radius tubular light-guide could degrade the 95% reflectivity specified for our Alzak material. However, as indicated in Fig. 2, which compares measured and simulated [3] photon transmission in a 19 mm diameter tube of varying length, this concern was unfounded: a reflectivity of 93% gives excellent agreement between experiment and theory.

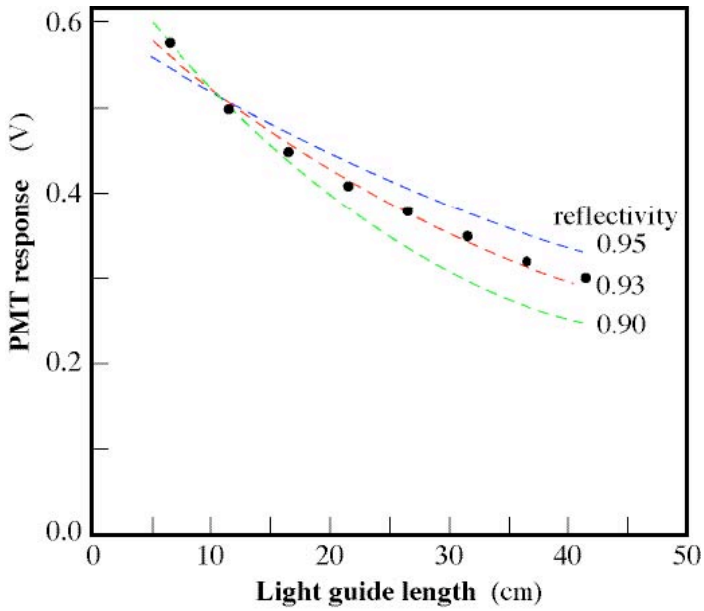

Fig. 2. Relative transmission of light through a 19 mm diameter tube lined with reflective Alzak material. The light from a blue-light emitting diode into a 30° cone was reflected from various lengths of the Alzak tube and measured using a photomultipler tube (pmt). The points are data; the lines represent the results of simulations with different reflectivity values.

Figure 3 shows the simulated Cerenkov light collection as a function of light guide diameter and cone opening angle. Only photons in the wavelength range 350–440 nm were considered, corresponding to a quantum efficiency of ≥ 25% for most photocathode materials. The photons were assumed to undergo specular reflection within the light-guide cone and tube until they reached the pmt entrance window located 50 cm from the radiator. Photons that struck the pmt window at large angles of incidence failed to be transmitted through to the photocathode.

As expected, for small tube diameters the calculated collection efficiency drops due to the large number of reflections required for propagation along the full length of the tube. The light collection generally has a broad maximum for cone opening angles of 35°–60°.

Although large matching light guide and pmt diameters favor high collection efficiency, they also make the detector more susceptible to background arising from the flux of particles traversing the light guide between the radiator and pmt photocathode, as well as to secondary radiation interacting directly in the pmt photocathode. In part, the corresponding signal-to-background ratio may be quantified by the ratio of the collection efficiency to the volume of the light guide or pmt window. An equivalent figure-of-merit, indicated in Fig. 4, is the collection efficiency divided by the square of the light guide or pmt diameter. The corresponding ratio is seen to be optimal for a pmt diameter close to that of the 19 mm diameter tube used for our light guide. Somewhat different models for the background generation do not significantly alter this conclusion.

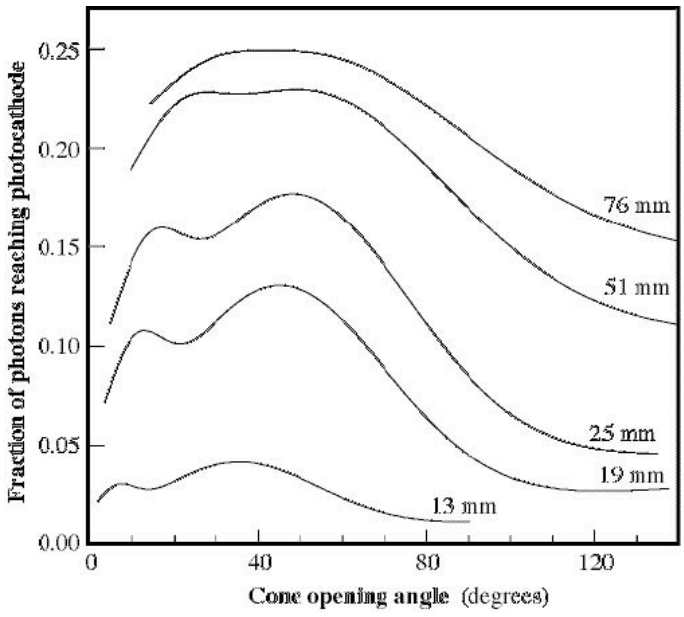

Fig. 3. Dependence of simulated light transmission on opening angle of mirror cone and diameter of a 50-cm long reflective tube. The calculations are for the wavelength range 350–440 nm.

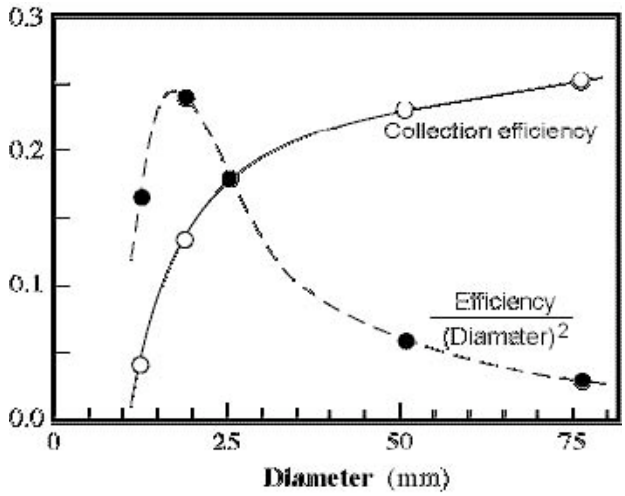

Fig. 4. Open points: Collection efficiency versus tube diameter for light propagation along a 50 cm-long tube. Solid points: Collection efficiency divided by tube diameter squared, arbitrarily normalized. This ratio constitutes a figure-of-merit for the signal-to-background ratio, where the background is produced either within the light guide tube, or in the pmt entrance window.

Cerenkov and scintillation photons produced in the air contained within the light guide constitute most of the background. In contrast to the Cerenkov photons that are radiated at an angle of only 1.4° in air relative to the initial electron direction, scintillation photons are isotropically distributed. Using results of ref. [4], one can estimate that a minimum ionizing particle passing through one cm of air produces about 0.0066 photons/sr in the wavelength range matching the photomultiplier cathode sensitivity. Assuming a 2π sr solid angle of photon collection in the 19 mm diameter reflective-tube and the 1.5 cm average path of the electron traversing it, yields one scintillation photon reaching the pmt per about 20 passing electrons. This number should be compared with about 200 Cerenkov photons reaching the pmt per electron passing through the radiator (see Fig. 6). Therefore under condition of uniform illumination, each cm of the tube would contribute about 0.06% to the signal from the Cerenkov light produced within the radiator. This number is sufficiently low to assure that even with an electron flux density varying by two orders of magnitude, the scintillation contribution from air in the light guide will not exceed a few percent.

Due to the small angle of Cerenkov photons produced in air, Cerenkov radiation produced within the light guide was of little concern over most of the length of the light guide tube: these photons just reflect back and forth, transverse to the tube axis.

On the other hand, Cerenkov photons produced within the reflective cone adjacent to the radiator are not similarly trapped; such photons may–with just one or two reflections–enter the pmt window. Figure 5 shows the results of simulations of Cerenkov production in the radiator and in the air-core light guide under uniform

electron flux irradiation for two light-guide diameters, 19 and 51 mm, assuming identical 5 x 5 x 20 mm^3 radiators of fused silica. As indicated, the larger diameter tube has a collection-efficiency for light produced in the radiator that is better by a factor of two. However, due to the much smaller air volume within its cone, the background produced within the light-guide of the 19 mm diameter tube is smaller by about two orders-of-magnitude–a striking improvement of scanner flux profile resolution, well-worth the cost of the reduced signal in the narrower tube.

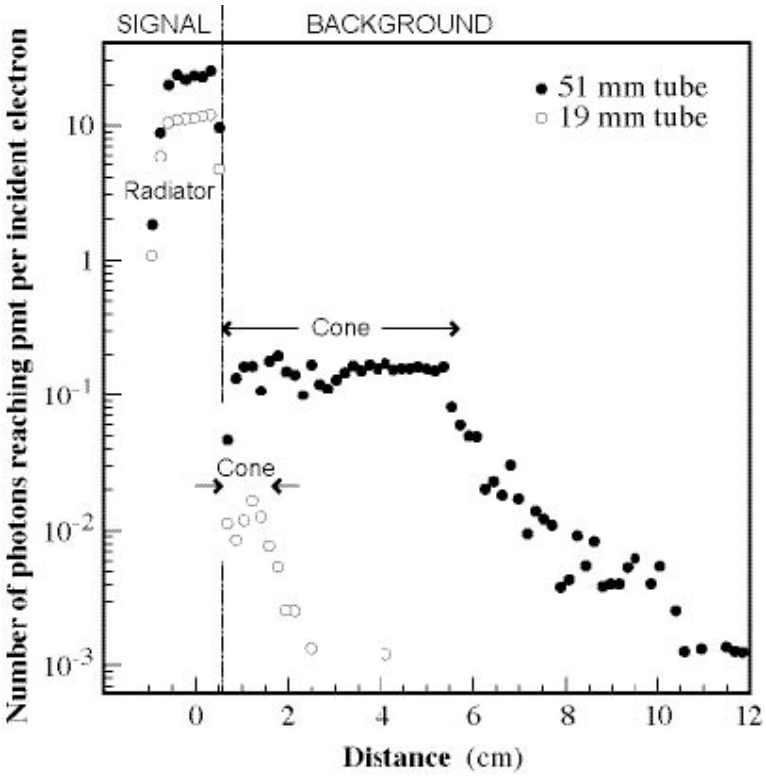

Fig. 5. Results of simulations showing the position of origin of Cerenkov photons that reach a pmt at the end of a 50 cm-long light guide tube for two different tube diameters. The reflectivity of the tube is assumed to be 93%. The solid (open) points are for a tube of internal diameter of 51 mm (19 mm).

As indicated in Fig. 6, the addition of the tungsten pre-radiator immediately upstream of the fused quartz radiator makes the detector much more responsive. The signal-to-background ratio is similarly improved. In addition, the pre-radiator enhances the directionality of the detector response, making it relatively insensitive to electron back-splash and other off-axis backgrounds.

Finally, Fig. 7 shows the uniformity of the light collection as a function of the Cerenkov production position within the radiator.

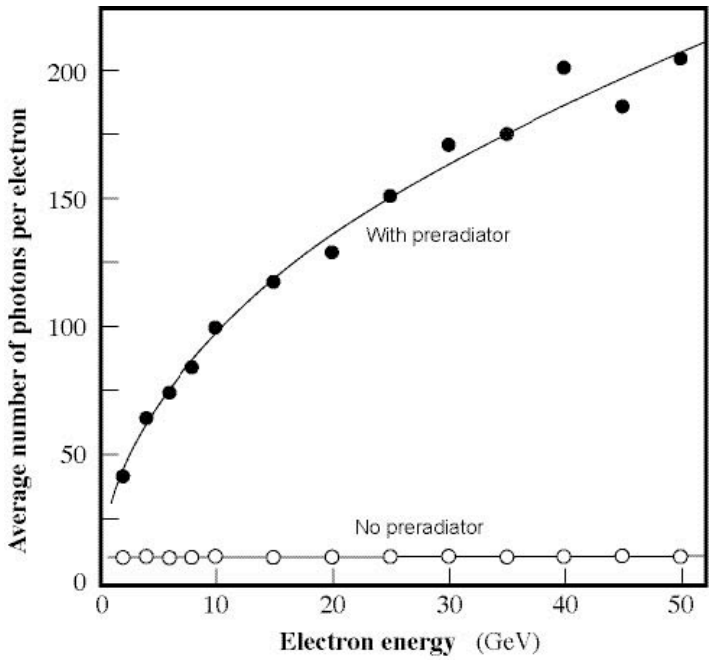

Fig. 6. Results of simulations for a 50 cm-long, 19 mm-diameter tube, with and without a five radiation-length pre-radiator. The ordinate is the number of photons reaching the pmt per incident electron striking the pre-radiator.

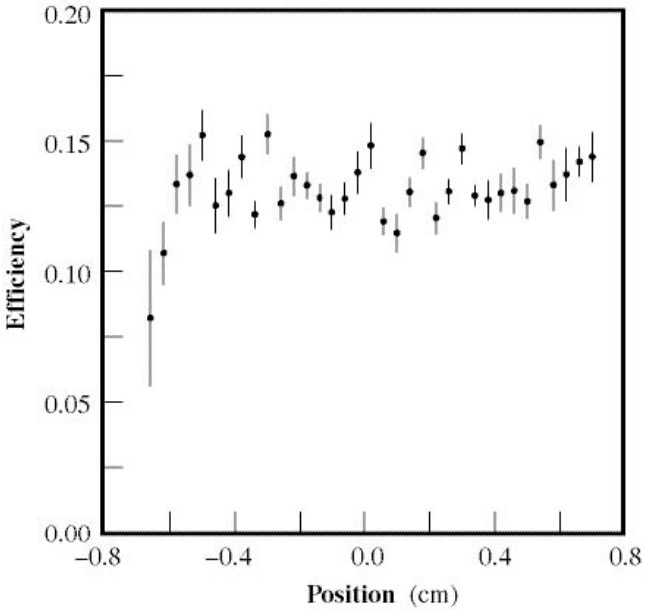

Fig. 7. Light collection efficiency as a function of interaction position in quartz radiator. The position shown is the projection along the light-guide axis.

2.2 Construction

Figure 8 shows the final version of the scanning Cerenkov detector that was built for experiment E158. Cerenkov light was produced in a fused silica radiator measuring 5 x 5 x 20 mm^3, canted at an angle of 45° to the incoming electron beam. As noted above, the 45° alignment of the quartz with respect to the beam served to optimize the response of the Cerenkov detector to the incoming beam and reduce sensitivity to background. Due to the high intensity of the scattered beam, the pmt that collects this Cerenkov light was situated just outside the E158 phase-space, about 50 cm from the radiators.

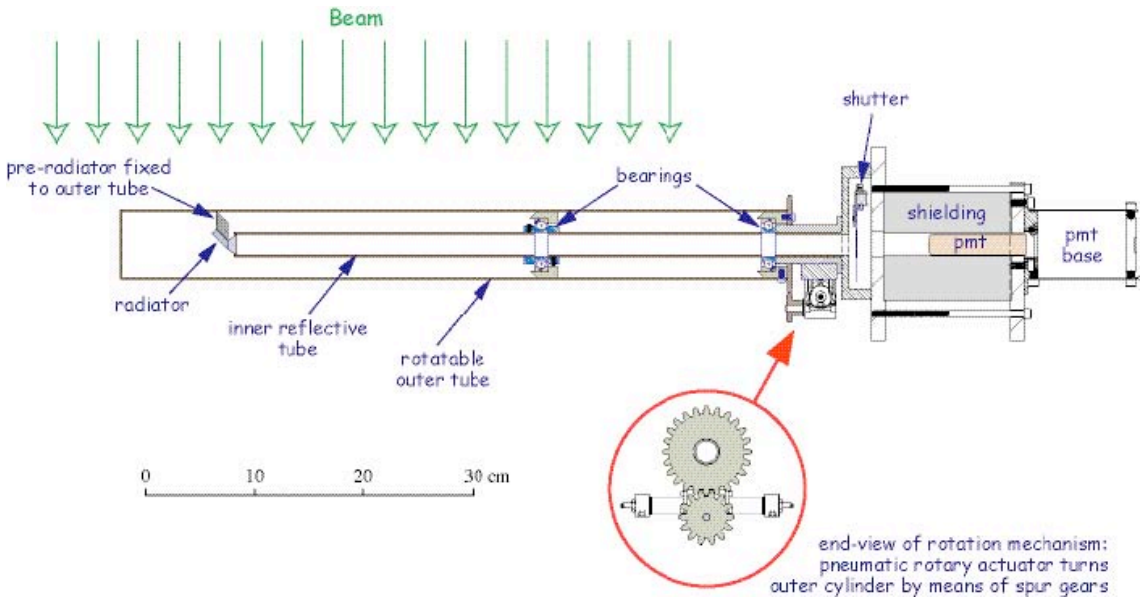

Fig. 8. Final design for measuring spatial distribution of an intense, broadly distributed electron-beam. In order to help identify and quantify background, a rotary actuator can move the pre-radiator to a position immediately downstream of the fused quartz radiator. The background is also reduced by surrounding the pmt with sintered tungsten shielding.

The inner tube was aluminum, with an inner diameter of 20.5 mm and a wall thickness of 0.08 mm. It was lined with a rolled sheet of Alzak–surfaced aluminum. The sheet we used was difficult to roll because it was 0.3 mm thick; if available, thinner stock would be preferred.

The electromechanical shutter [5] had a circular aperture of 25.4 mm. Normally the shutter was open, but when closed it allowed us to check for background generated by stray ionizing radiation directly hitting the 19 mm–diameter pmt [6]. In order to reduce this background the sides of the pmt were shielded by 4 cm of tungsten.

Just recently we constructed a similar detector for use in theHappex II experiment at the Thomas Jefferson National Laboratory [7]. In contrast to the low duty-cycle, high pulse intensity beam used in the E158 experiment, in the HAPPEX experiment a

continous beam of scattered electrons was detected inside a shielded spectrometer hut, an environment with a much lower radiation level than existed for E158 at SLAC. Consequently, the detector design was simplified by omitting the heavy tungsten shielding around the pmt, as well as the mechanism for removing the pre-radiator from the upstream side of the fused silica radiator. To compensate for lower intensity of countinuous beam, a higher gain XP2982 phototube [8] was used.

2.3 Motion

As described above, in experiment E158 the electrons scattered from the protons and from the electrons in the hydrogen target formed two concentric circular bands surrounding an intense forward-directed bremsstrahlung background. In order to scan the two bands, Cerenkov detectors were positioned 90° apart on a rotatable annulus of outer diameter 246 cm as shown in Fig. 9. The detectors were mounted on four linear movers [9] so that they could be moved radially relative to the beam axis. The annulus could be rotated through an angle of 220°thus allowing the entire profile of the scattered electrons to be measured. In order to avoid beam interception during the experimental runs, the Cerenkov detectors were moved to a radial position beyond the scattered electron beam.

The annulus [10] had an outside aluminum rim of 44 mm radial thickness and 108 mm depth onto which was welded a 6 mm thick circular aluminum plate. For ease of transport and flexibility in assembly, it separated into two halves joined together by fish plates and by tension blocks welded under the rim. The annulus was entrapped and supported by a pair of large brass bearing wheels, and was rotated by means of turning a sprocket wheel that engaged a roller chain fixed in a groove machined into the edge of the rim. The sprocket wheel itself was driven through a 20:1 reduction gear by a stepping motor mounted on the support frame for the annulus. When assembled at SLAC with its full complement of detectors, the roundness of the annulus was measured to be better than 0.25 mm.

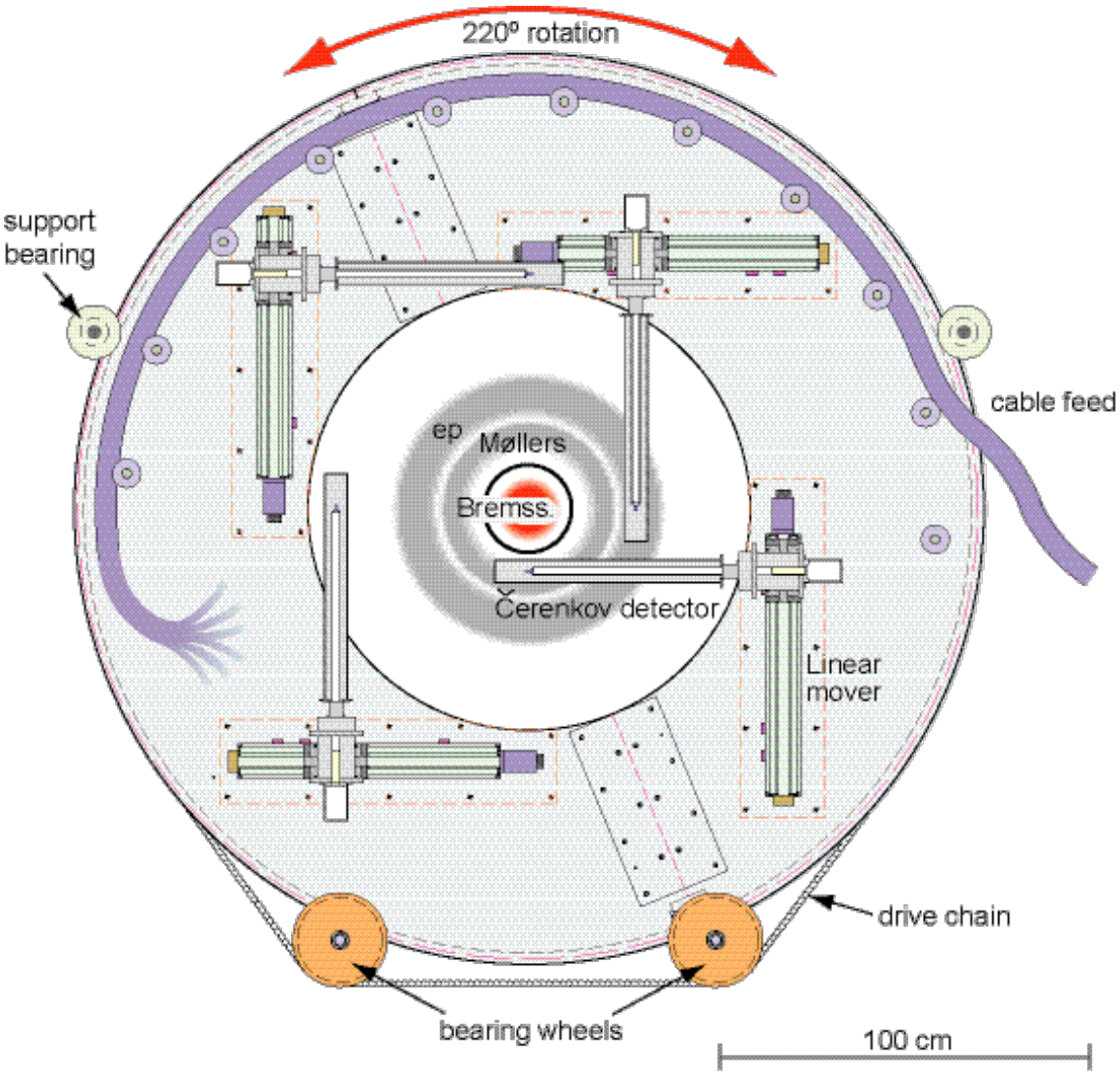

Fig. 9. Arrangement of four Cerenkov detectors on rotatable annulus. Linear movers translate the detectors radially, while the annulus can be rotated 220° by means of chain embedded in its rim. The annulus was supported on two large brass bearing wheels, and stabilized in the vertical plane by smaller bearings at about 2/3 of the annulus height. The entire system was enclosed by a frame attached to a moveable cart that also provided earthquake protection. High-voltage, signal, and motion control cables were bundled on both sides around the perimeter of the annulus, and held on hangers at 15° intervals so as to accommodate the cable transport through the full 220° rotation of the annulus. During experimental runs a tungsten–lead collimator was installed to intercept electrons scattered from the protons.

The annulus rotation and the linear translation of the Cerenkov scanners were remotely controlled by means of a LabView Flexmotion [11] application. The Cerenkov scanners were equipped both with optical rotary encoders for the motion control, and with linear potentiometers [12] for providing position information into the data acquisition system.

2.4 Performance

The scanner system worked well throughout the two-year period of this experiment. Apart from the commissioning periods when it was used extensively, the scanner was typically used for beam profile checks about twice each day. Despite the large integrated luminosity of this experiment, no degradation was observed in the scanner performance. Fig. 10 shows the result of a typical radial scan.

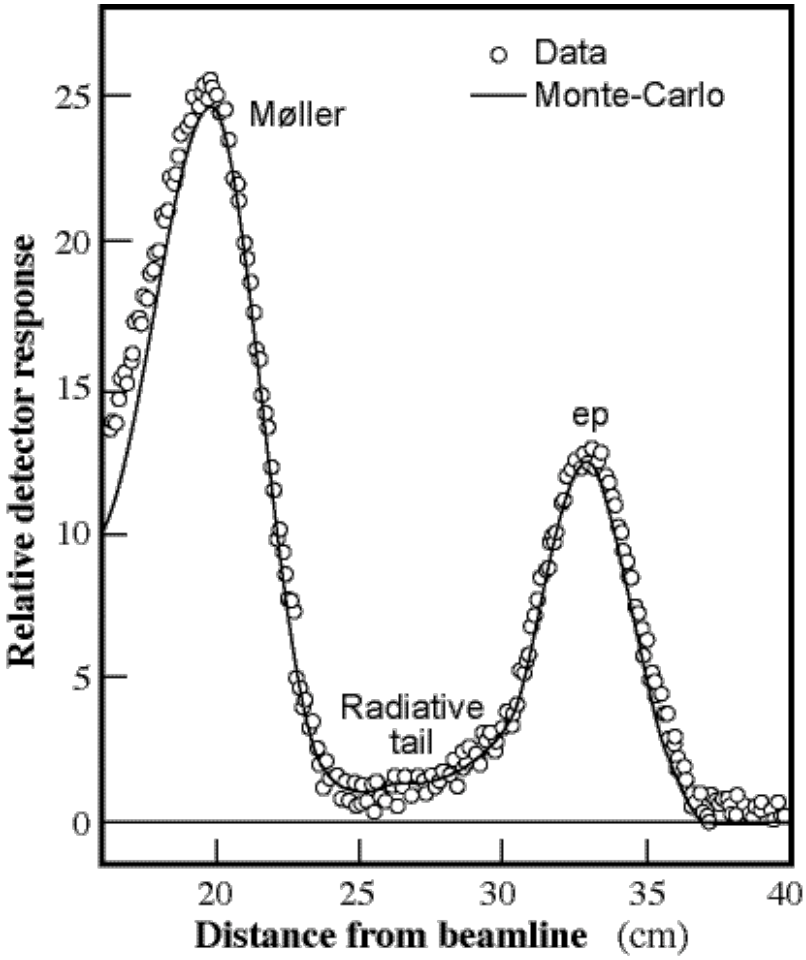

Fig. 10. Radial response of scanning Cerenkov detector, and comparison to normalized Monte carlo prediction.

3. Cerenkov Polarimeter

3.1. General

In experiment E158 the polarization of the incident electron beam was determined by measuring Møller scattering from magnetized iron foils mounted at 20^0 with respect to the beam and ranging in thickness between 20 and 100 μm. For such thin targets, the Møller count rate was reduced by a factor of ≈ 200 compared to the rate from the 1.5-m long liquid hydrogen target used in the experiment. In order to eliminate the (e,p) background and define a certain kinematics acceptance, a collimator was used which limited the scattered beam to area of a size of 7 x 1 cm^2 in the detector plane. The Moller calorimeter was not suitable for polarimetry measurements because its size and geometry did not match the collimator geometry. On the other hand, the reduction of the scattered flux intensity would have made it difficult to acquire the desired precision with the small scanning Cerenkov detector described in Section 2.

Hence a second air-core detector was designed that featured a much larger and thicker active element. Nevertheless, the overall concept for this polarimeter was similar to that of the smaller air-core Cerenkov scanners. As shown in Fig. 11, the air-core light guide of the polarimeter was a 10 cm internal diameter tube whose internal surface was lined with Alzak [2]. Cerenkov photons were reflected around a 90° angle in the tube by means of an Alzak-surfaced rotatable mirror that could be set to bisect the angle between the horizontal and vertical tubes. This arrangement has two benefits. First, by rotating the mirror 180° about a vertical axis, Cerenkov photons that would normally be reflected towards the pmt were obstructed. This allowed a measurement of the background due to radiation interacting directly in the pmt. Effectively then, the rotatable mirror served the same function as the shutter in the scanning Cerenkov detector. The second feature, a significant improvement over the more compact Cerenkov scanner, is that the 90° angle in the light-guide permitted the photocathode of the pmt to be shielded from line-of-sight background originating in the vicinity of the beam pipe. In our case the shielding was provided by 10 cm of lead surrounding the detector.

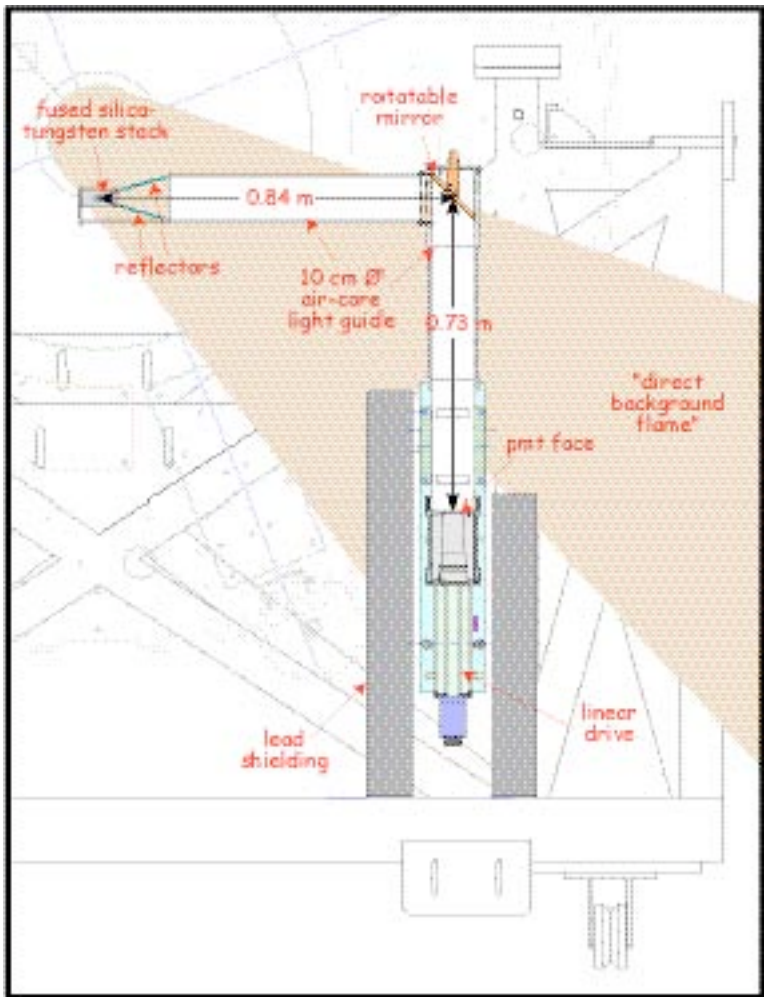

Fig. 11. Air-core Cerenkov detector installed on detector cart and used for polarimetry in experiment E158 at SLAC. Driven by a linear mover, the fused silica-tungsten detector head can be moved vertically through a band of scattered electrons beneath the beam-axis. Ten cm of lead shielded the PMT from line-of-sight background produced in the vicinity of the beam-pipe.

The active element of the polarimeter consisted of alternating layers of fused silica and tungsten of total thickness of 13 radiation lengths. Due to the massive calorimetric construction of this active element, we did not try to build in the capability of remote removal of the high-Z tungsten pre-radiator, as for the Cerenkov scanner.

3.2 Design

The transverse size of the active element was optimized to match the 7 x 1 cm^2 image produced by special spectrometer optics used in the polarimetry measurements. In order to allow for the transverse development of the electromagnetic shower within the detector, the size of the fused silica-tungsten stack was made slightly larger than this. Each of the six fused silica plates measured 9.3 x 3.5 x 0.6 cm^3, and the tungsten plates, 7 in all, 9.8 x 3.5 x 0.6 cm^3. As shown in Fig. 12, this stack was tilted relative to the beam by 30°, an angle calculated to optimize the response of the detector. The calculated dependence on angle is shown in Fig. 13.

Extensive GEANT [3] Monte-Carlo calculations were made to optimize the details of the detector. These calculations guided the choice of the number and thicknesses of the fused silica and tungsten layers, as well as their orientation relative to the beam. In addition to the Alzak lining of the light-guide tube, the simulations also favored the use of reflective surfaces elsewhere in the detector. For example, calculations showed that reflective foils laid against each fused silica plate increased the response of the detector by about 30%. The simulations also showed the efficacy of two planar reflectors, semi-elliptical in shape, installed above and below the detector element at an angle of 15° to the tube axis. Cerenkov photons emerging from the fused silica layers were reflected by these Alzak reflectors such that they followed paths more parallel to the axis of the air-core light guide. This reduced the number of reflections each ray underwent, thus improving the light collection.

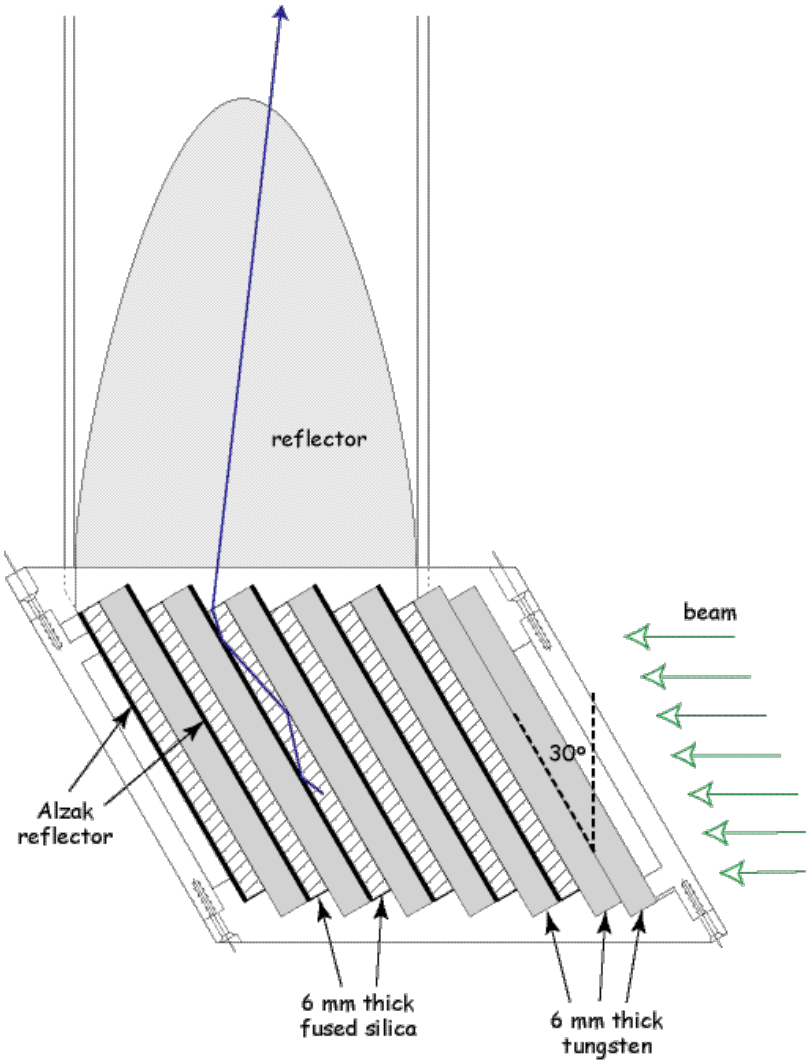

Fig. 12. Arrangement of tungsten and fused silica layers in the active element of the air-core polarimeter. Cerenkov photons generated by the electromagnetic shower reflect along the fused silica layers and emerge from the top. In the plane normal to this view, the photons are reflected close to the axis of the air-core light guide by two planar semi-elliptical reflectors, one above and the other below the detector elements. Alzak foils placed against each fused silica plate increased the response of the detector by about 30%.

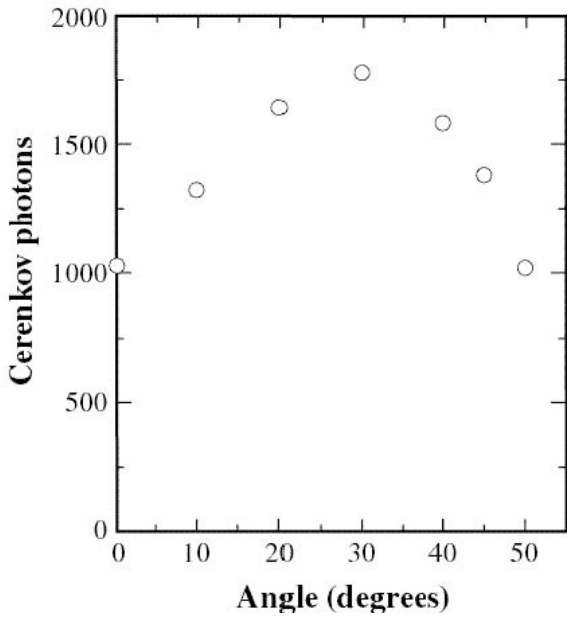

Fig. 13. Calculated number of Cerenkov photons in the air-core light-guide, for a single 22 GeV electron showering in the detector stack. The response is calculated as a function of the angle between the incident beam and the normal to the fused silica-tungsten stack.

The adopted design provided not only large signal strength, but also the necessary energy resolution to discriminate against low energy backgrounds. As indicated in Fig. 14, the response of the calorimeter is also reasonably linear in a range of 10-100 GeV, though the relative signal drops considerably for low and for high energies. The drop at low energies aids in reducing background.

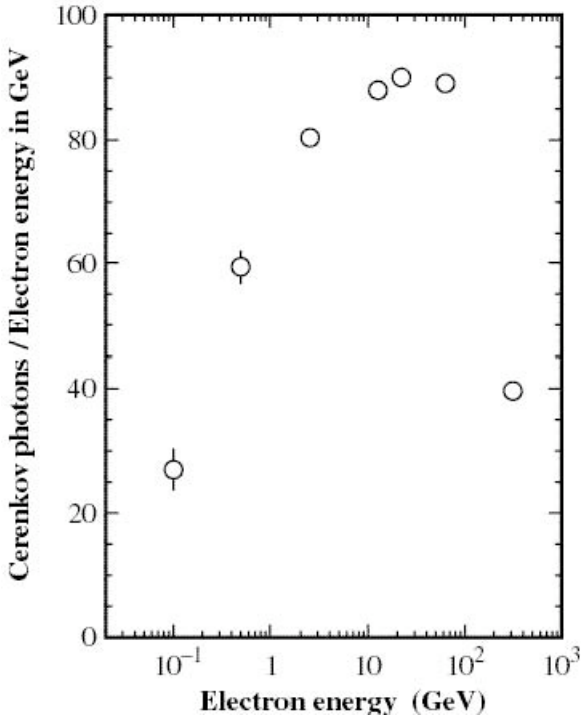

Fig.14. Monte Carlo results for dependence of detector response on electron energy. The response is quite linear for the 20–30 GeV energy-range of Møller-scattered electrons in experiment E158.

Figure 15 shows two perspectives of the simulated response of the detector to the absorption of a 22 GeV electron. No shower products are shown other than the Cerenkov photons. Moreover, for clarity, only 0.5% of the expected number of photons were simulated.

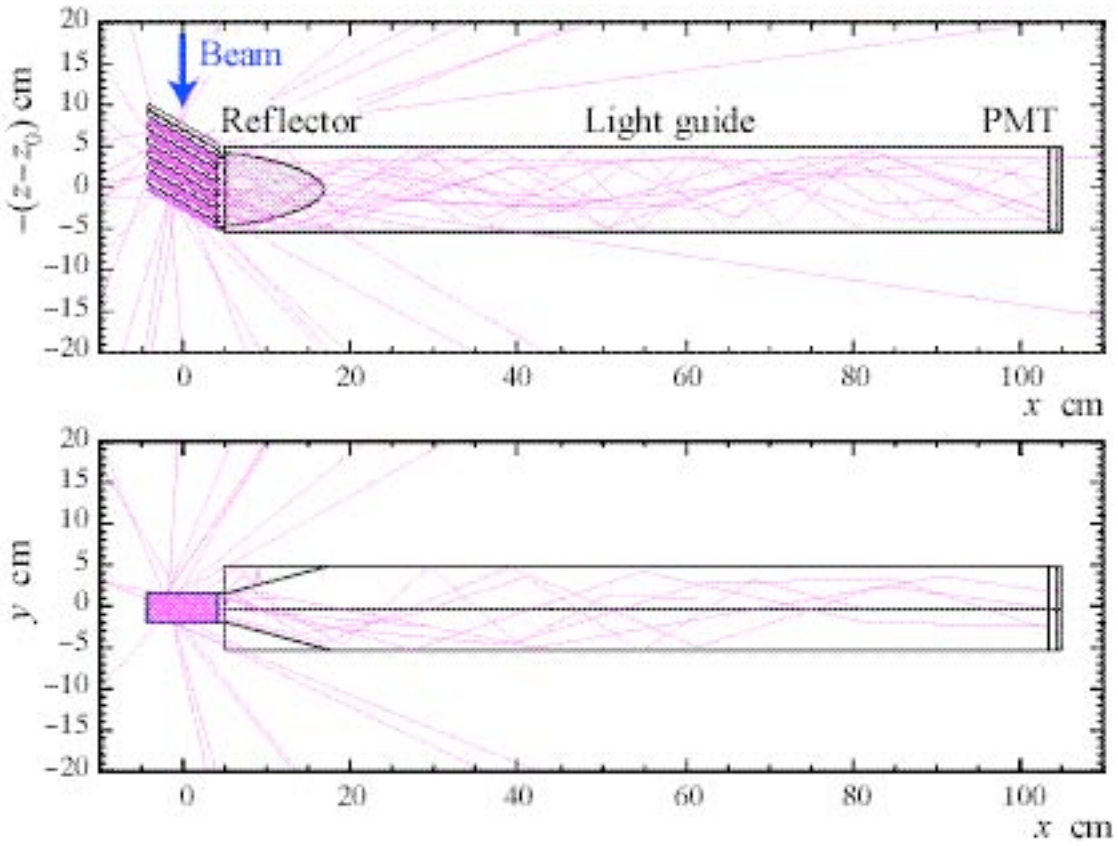

Fig.15: Monte Carlo simulation showing 0.5% of Cerenkov photons produced by the showering of a single 22 GeV electron in the air-core polarimeter.

The simulations, for a 1-m long straight air-core light guide with a 10 cm internal-diameter and a 10 cm phototube indicated that about 1800 Cerenkov photons reach the pmt for every 22 GeV Møller electron absorbed in the detector. Because the constructed light guide was 1.6 m long with a 90° bend, and a 5 cm Hamamatsu pmt [13] was used, in practice, the yield was considerably lower. Moreover, the window material of the pmt was *not* of a type that favors high ultraviolet transmission, and hence a fraction of the Cerenkov photons were absorbed before reaching the pmt photocathode. However, these losses were considered acceptable in view of the very large flux of Møller-scattered electrons (*quantitative value?*) incident upon the polarimeter.

3.3 Some practical information

The rotatable mirror was fabricated by bolting a 6.3 mm thick brass plate to the 45°–beveled end of a 33 mm diameter aluminum shaft. By turning the shaft in a lathe, the plate was machined to the required elliptical profile. An Alzak foil was fixed to the brass plate to provide the reflective surface. The assembly was rotated by a 180° pneumatic actuator [14], and limit switches were added to indicate the mirror position.

When not in use, the polarimeter was moved outside of the scattered beam region. As for the Cerenkov scanners, this motion through a radial distance of 0.5 m, was provided by a Parker-Daedal 404XR linear mover [9] equipped with limit and home switches, and rotary and linear position encoders. The square rails of the linear mover were well-suited for resisting the appreciable torque imposed by the 5 kg of tungsten supported a distance of 85 cm off to the side of the mover's axis.

As with the Cerenkov scanners, the motion of the polarimeter was controlled by a National Instruments Flexmotion [11] with its linear potentiometer providing position information to the data acquisition system.

3.4 Performance

Figure 16 shows results for two radial scans for an unpolarized carbon target. One scan was made with the mirror set for transmission, the other for the mirror obstructing Cerenkov photons. This lack of a sizeable signal in the obstructed case confirms that background due to radiation interacting directly in the pmt was insignificant.

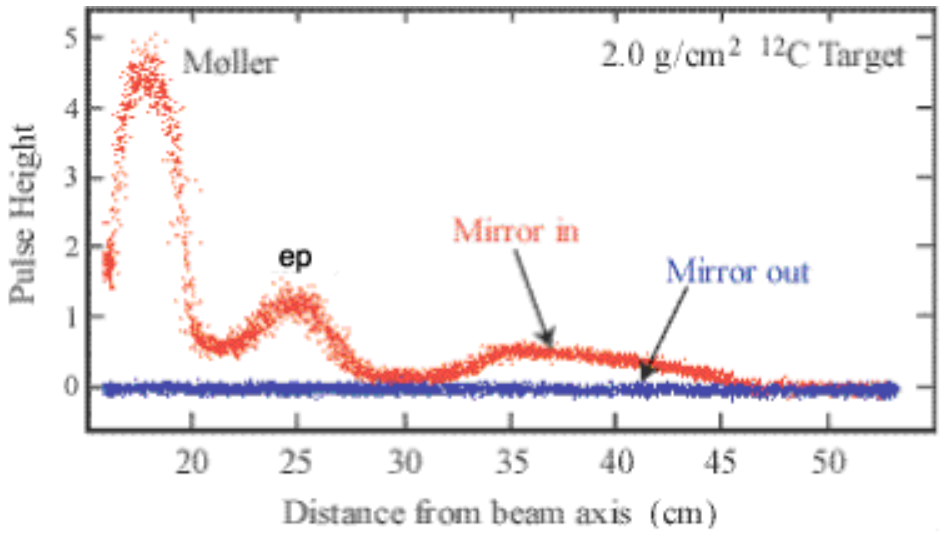

Fig. 16. Potentiometer response measured as a function of radial distance from the beam axis. In the "Mirror in" position the mirror reflects Cerenkov light produced in the calorimeter to the pmt. In the "Mirror out" position this light is obstructed.

Figure 17 shows the polarimeter response distribution obtained using a polarized foil. In one case the beam polarization is aligned with the polarization of target electrons, (total helicity 1), in the other case the polarizations are opposite (total helicity 0). The response is normalized according to the charge in each accelerator beam pulse, as measured by a toroidal coil. The difference in responses arises from the dependence of the Møller cross section on the total helicity. The data were used to determine the extent of the polarization of the incident electron beam. In our case this ranged from 80–90%, with a statistical uncertainty of about 4% for a 20 minute run.

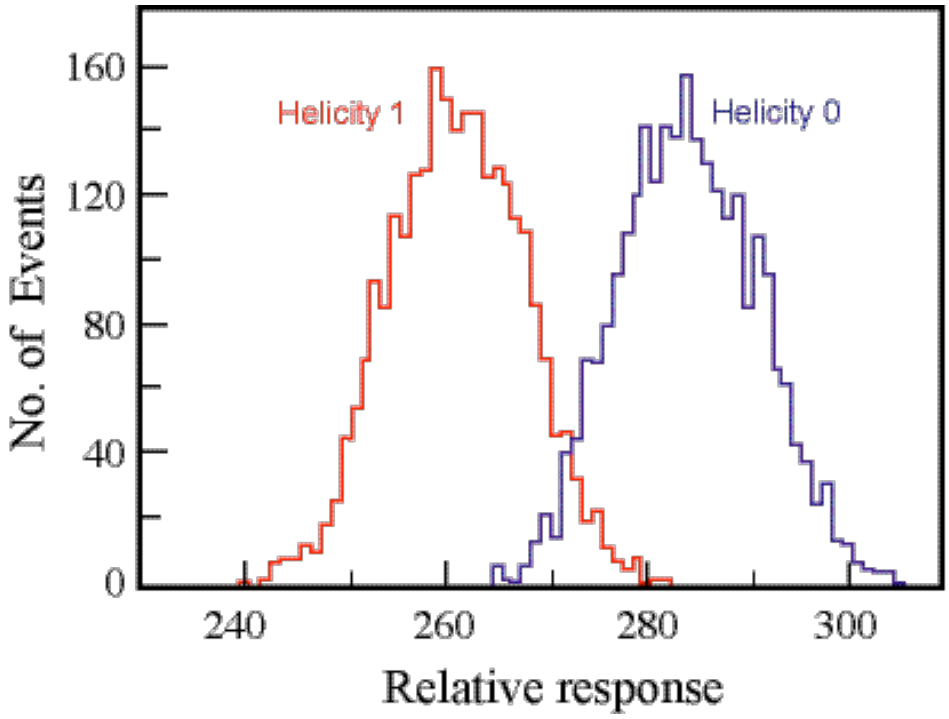

Fig. 17. Pulse-height distributions of polarimeter pulses for helicity 0 and helicity 1 Møller scattering. Each polarimeter pulse is integrated over one beam pulse, and in this plot normalized according to the total charge in the beam pulse as measured by a toroid. Note the suppressed zero on the abscissa.

References

[1] SLAC proposal E158: "A Precision Measurement of the Weak Mixing Angle in Møller Scattering", K. Kumar *et al*. (1997). (http://www.slac.stanford.edu/grp/rd/epac/Proposal/E158.pdf), P.L. Anthony *et al.*, Phys. Rev. Lett., **92**, 181602 (2004).

[2] MIRO 2, ALANOD Aluminium-Veredlung GmbH & Co. KG, Germany. Alzak Registered is trademark of the Aluminum Company of America (ALCOA).

[3] GEANT v. 3.21, CERN Program Library.

[4] S. Bertolucci *et al.*, "Scintillation in Gases Commonly Used as Cerenkov Radiators", DESY preprint 75/16, July 1975.

[5] Uniblitz© shutter. Vincent Associates, Rochester N.Y., USA.

[6] Thorn EMI, model 9083A. Electron Tubes Limited, Ruislip, Middlesex, England.

[7] Happex II, Jefferson Lab. Proposals E99-115 (Spokespersons: K. Kumar, D. Lhullier and G. Cates, 1999). and E00-114 (Spokespersons: D. Armstrong and R. Michaels, 2000).

[8] Photonis, model XP2982, LANCO International, Inc., Rosswell, GA, USA.

[9] Parker-Daedal, model 404XR.

[10] Fabricated to our specifications by Western Mass Machining, of Holyoke, Massachusetts.

[11] National Instruments, Inc. Austin, TX, USA.

[12] Unimeasure Inc., Corvallis, OR, USA.

[13] Hamamatsu Photonics K.K. 2 inch photomultiplier, model R2154-02. Hamamatsu City, Japan.

[14] Bimba Manufacturing Company, Monee, IL, USA.